frontiers | Frontiers in Energy Research

TYPE Original Research
PUBLISHED 22 August 2022
DOI 10.3389/fenrg.2022.967307

OPEN ACCESS

EDITED BY
Umar Khan,
Hazara University, Pakistan

REVIEWED BY
Muhammad Sohail,
Institute of Space Technology, Pakistan
Zubair Ahmad,
University of Campania "Luigi Vanvitelli," Italy
Waseem Sikander,
The University of Haripur, Pakistan

*CORRESPONDENCE
Aatif Ali,
atifkh98@gmail.com

SPECIALTY SECTION
This article was submitted to Process and Energy Systems Engineering, a section of the journal Frontiers in Energy Research

RECEIVED 12 June 2022
ACCEPTED 15 July 2022
PUBLISHED 22 August 2022

CITATION
Alshahrani S, Ahammad NA, Bilal M, Ghoneim ME, Ali A, Yassen MF and Tag-Eldin E (2022), Numerical simulation of ternary nanofluid flow with multiple slip and thermal jump conditions.
Front. Energy Res. 10:967307.
doi: 10.3389/fenrg.2022.967307

Numerical simulation of ternary nanofluid flow with multiple slip and thermal jump conditions

Saad Alshahrani[1], N. Ameer Ahammad[2], Muhammad Bilal[3], Mohamed E. Ghoneim[4,5], Aatif Ali[6]*, Mansour F. Yassen[7,8] and Elsayed Tag-Eldin[9]

[1]Department of Mechanical Engineering, College of Engineering, King Khalid University, Abha, Saudi Arabia, [2]Department of Mathematics, Faculty of Science, University of Tabuk, Tabuk, Saudi Arabia, [3]Department of Mathematics, City University of Science and Information Technology, Peshawar, Pakistan, [4]Department of Mathematical Sciences, Faculty of Applied Science, Umm Al-Qura University, Makkah, Saudi Arabia, [5]Faculty of Computers and Artificial Intelligence, Damietta University, Damietta, Egypt, [6]Department of Mathematics, Abdul Wali Khan University Mardan, Mardan, Khyber Pakhtunkhwa, Pakistan, [7]Department of Mathematics, College of Science and Humanities in Al-Aflaj, Prince Sattam Bin Abdulaziz University, Al-Aflaj, Saudi Arabia, [8]Department of Mathematics, Faculty of Science, Damietta University, New Damietta, Damietta, Egypt, [9]Faculty of Engineering and Technology, Future University in Egypt, New Cairo, Egypt

This study addresses the consequences of thermal radiation with slip boundary conditions and a uniform magnetic field on a steady 2D flow of trihybrid nanofluids over a spinning disc. The trihybrid nanocomposites are synthesized by the dispersion of aluminum oxide (Al_2O_3), zirconium dioxide (ZrO_2), and carbon nanotubes (CNTs) in water. The phenomena are characterized as a nonlinear system of PDEs. Using resemblance replacement, the modeled equations are simplified to a nondimensional set of ODEs. The parametric continuation method has been used to simulate the resulting sets of nonlinear differential equations. Figures and tables depict the effects of physical constraints on energy and velocity profiles. According to this study, the slip coefficient enormously decreases the velocity field. For larger approximations of thermal radiation characteristics and heat source term boosts the thermal profile. This proposed model will assist in the field of meteorology, atmospheric studies, biological technology, power generation, automotive manufacturing, renewable power conversions, and detecting microchips. In regard to such kinds of practical applications, the proposed study is being conducted. This study is unique due to slip conditions and ternary fluid, and it could be used by other scholars to acquire further information about nanofluid thermal exchanger performance and stability.

KEYWORDS

slip conditions, thermal radiation, heat generating source, computational approach, ternary nanofluid, rotating disc

Introduction

Rotating disks are used in a wide range of engineering and industrial applications such as gas flywheels, spinning disk electrodes, turbine engines, brakes, and gears (Li et al., 2021; Zhou et al., 2021; Chu et al., 2022a). The modeling and simulation of ferrofluid flow with heat transfer induced by an irregular rotatable disc oscillating upward were investigated by Zhang et al. (2021). The wavy rotating material increases energy conversion by up to 15% as compared to a level surface. Waini et al. (2022) used the bvp4c MATLAB programming to investigate the chaotic flow over a gyrating disc in nanofluids with deceleration and suction features. Alrabaiah et al. (2022) investigated the flow of magnesium oxide, silver, and gyrotactic microbe-based hybrid nano composites within the cylindrical space connecting the disc and cone in the context of thermal energy stabilization. It was discovered that by combining a rotating disc with an immobile cone, the cone–disk system may be cooled to its desired temperature, whereas the outer edge system is in equilibrium. The flow of nanofluids across a preheated revolving disc has been computationally evaluated as a result of random motion, heat conduction, and thermal radiation by Chu et al. (2021a). They described many features of momentum and heat transformation using Arrhenius kinetic energy. The radiation and Prandtl number effect are thought to promote heat exchange while enhancing the magnetic component which lowers velocity distribution. Naveen Kumar et al. (2022) evaluated the nanofluid flow over a spinning, stretchy disc with an unsteady heat source. The heat transmission of both fluids accelerates as the ratios of temperature- and space-related heat supplier factors increase. Alhowaity et al. (2022) developed the energy transmission over a moving sheet. It was hypothesized that adding carbon nanotubes and nanoclusters to water improves its thermophysical and energy transport capabilities drastically. Sharma et al. (2022) proposed a spinning disc with temperature-dependent geothermal viscosity and thermal conductivity, causing the hydrodynamic flow of magnetized ferrofluid. Kumar and Mondal (2022) analyzed quantitatively the electrically radiating unsteady viscous fluid flow due to a stretchy spinning disc with an externally supplied magnetic field, looking at both descriptive and analytical aspects of heat transmission. Recently, many investigators have documented substantial involvement to the fluid flow across a rotating disc (Bilal et al., 2022a; Alsallami et al., 2022; Murtaza et al., 2022; Ramzan et al., 2022).

Hybrid and trihybrid nanofluids combine the metallic, non-metallic, or polymeric nano-size powder with a conventional fluid to maximize the thermal efficiency for a wide range of purposes such as, solar energy, refrigeration and heating, ventilation, heat transition, heat tubes, coolant in machines, and engineering. Many experiments have noted that hybrid nanofluids have a superior energy conduction rate than pure fluids, both experimentally and statistically (Khan et al., 2020; Alhowaity et al., 1002; Elattar et al., 2022). The working fluid in this study contained Al_2O_3, ZrO_2, and CNT. Sahu et al. (2021) analyzed the free convection steady-state and loop's transient features utilizing a variety of water-based trihybrid (Al2O3 + Cu + CNT/water) nanofluids. Ramadhan et al. (2019) examined the instability of trihybrid nanofluids. The tri-hybrid nanocomposite was successfully synthesized and displayed excellent compatibility. Muzaidi et al. (2021) addressed the physical parameters (crystallite size, surface shape, and density) of $SiO_2/CuO/TiO_2$ trihybrid nanofluids. The trihybrid solution exhibited the best thermal characteristics, based on thermal production, at roughly 55°C. Al-Mubaddel et al. (2022) documented the model for generalized energy and mass transfer comprising magnetized cobalt ferrite. The influence of permeability factor, inertial element, and buoyant ratio on the fluid velocity has been reported, while the temperature conversion curve improves dramatically with the increasing values of Eckert number, Hartmann number, and heat absorption/generation. Ullah et al. (2021); Ullah et al. (2022) used an elongated substrate to describe the convective flow of Prandtl–Eyring nanofluids, taking into account the important factors including activation energy, chemical reaction, and Joule heating. Safiei et al. (2021) used a newly created metal fabrication fluid called ZrO_2-SiO_2-Al_2O_3 trihybrid ferrofluid in the cutting zone to produce a good surface quality on manufactured items while also reducing the cutting forces. Gul and Saeed (2022) worked on improving thermal flow for trihybrid nanofluid flow across a nonlinear extending plate. It was discovered that as the volumetric fractions of NPs enhance the nonlinearity index of the sheet and velocity profile decreases. Lv et al. (2021) examined the Hall current and the heat radiation effect on hybrid nanofluid flow over a whirling disc. Their endeavor was motivated by the desire to improve the thermal energy transmission for mechanical and manufacturing uses. The heat transfer rate decreases with Hall current and increases with the radiative component, according to the findings. Palanisamy et al. (2021) investigated the characterization and thermophysical characteristics of trihybrid oxide nanostructures, including SiO_2, TiO_2, and Al_2O_3, produced at 0.1 per concentration in three distinct ratios. Furthermore, many scholars have reported on the uses and applications of ternary nanofluid (Sohail et al., 2019; Ahmed et al., 2020a; Sohail et al., 2020a; Ahmed et al., 2020b; Chu et al., 2021b).

When viscosity effects at the wall are insignificant and mesh size is substantially larger than the boundary layer thickness, the slip wall condition is used. Hussain (2022) statistically and numerically assessed to capture the flow characteristics of hybrid nanofluid flow across an enormously extensible sheet with thermal and velocity slip conditions. The results show that a little increase in the thermal slip factor generates a significant change in the thermal transfer rate when compared to the radiation impact. Swain et al. (2022) addressed the uniform chemical reaction and magnetic field effect on the water-based hybrid nanofluid passing over a dwindling permeable sheet with slip boundary conditions. The suction and injection component enhances the skin friction ratio; however, the velocity slip factor has the opposite trend. Ullah (2022) demonstrated the flow of a hydromagnetic hybrid nanofluid in a 3D nonlinear convection layer in the existence of microorganisms and different slip circumstances across a slandering substrate. Many scholars have recently hugely reported on thermal and velocity slip conditions (Khan et al., 2017; Sohail et al., 2020b; Ahmed et al., 2020c; Saeed et al., 2021; Algehyne et al., 2022).

The purpose of this research is to elaborate the consequences of slip boundary conditions on ternary hybrid nanofluid flow in the presence of heat source and thermal radiation over a rotating disc. The thermophysical properties of ternary nanoparticles (Al_2O_3, ZrO_2, and CNT) and base fluid (H_2O) are investigated in this study. To numerically resolve the dimensionless system of ODEs, the parametric continuation method has been applied using MATLAB's software. The current study's unique findings are useful and valuable in academic studies and other fields.

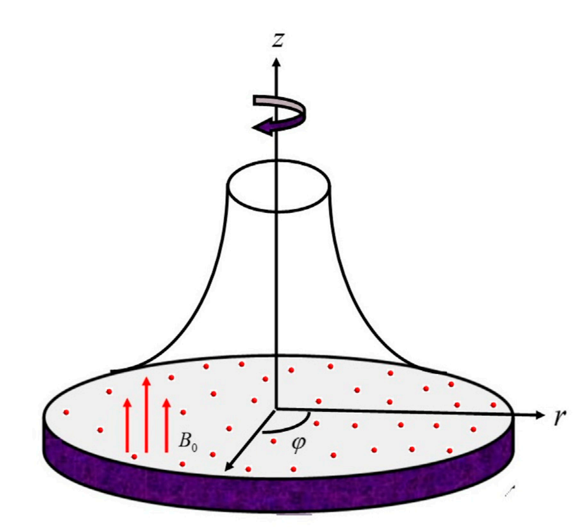

FIGURE 1
Ternary hybrid nanofluid flow over a rotating disc.

Mathematical formulation

A steady two-dimensional trihybrid nanofluid flow with nano composites (Al_2O_3, ZrO_2, and CNT) over a disc in the presence of thermal radiation and slip boundary conditions is studied. The (r, ϕ, z) cylindrical coordinate system is considered as elaborated in Figure 1. The disc rotates with fixed angular velocity Ω. The magnetic field B_0 is applied in the axial direction of fixed intensity. Moreover, we can ignore the induced magnetic field by considering low magnetic Reynolds number. T_w and T_∞ are the wall and ambient temperature of fluid, respectively. Based on abovementioned postulation, the elementary phenomena are modeled as (Iqbal et al., 2021):

$$\frac{\partial u}{\partial r}+\frac{u}{r}+\frac{\partial w}{\partial z}=0, \tag{1}$$

$$\rho_{tnf}\left(u\frac{\partial u}{\partial r}+w\frac{\partial u}{\partial z}+\frac{v^2}{r}\right)=-\frac{\partial P}{\partial r}+\mu_{tnf}\left(\frac{\partial^2 u}{\partial r^2}-\frac{u}{r^2}+\frac{1}{r}\frac{\partial u}{\partial r}+\frac{\partial^2 u}{\partial z^2}\right)-\sigma_{tnf}B_0^2 u, \tag{2}$$

$$\rho_{tnf}\left(u\frac{\partial v}{\partial r}+w\frac{\partial v}{\partial z}+\frac{uv}{r}\right)=\mu_{tnf}\left(\frac{\partial^2 v}{\partial r^2}-\frac{v}{r^2}+\frac{1}{r}\frac{\partial v}{\partial r}+\frac{\partial^2 v}{\partial z^2}\right)-\sigma_{tnf}B_0^2 v, \tag{3}$$

$$\rho_{tnf}\left(u\frac{\partial w}{\partial r}+w\frac{\partial w}{\partial z}\right)=-\frac{\partial P}{\partial z}+\mu_{tnf}\left(\frac{\partial^2 w}{\partial r^2}+\frac{1}{r}\frac{\partial w}{\partial r}+\frac{\partial^2 w}{\partial z^2}\right), \tag{4}$$

$$\left(\rho C_p\right)_{tnf}\left(u\frac{\partial T}{\partial r}+w\frac{\partial T}{\partial z}\right)=k_{tnf}\left(\frac{\partial^2 T}{\partial r^2}+\frac{\partial^2 T}{\partial z^2}+\frac{1}{r}\frac{\partial T}{\partial r}\right)-q_{rz}+Q_0\left(T-T_\infty\right), \tag{5}$$

where

$$q_r=\frac{-4\sigma^*}{3k^*}\frac{\partial T^4}{\partial z}=\frac{-16\sigma^*}{3k^*}T^3\frac{\partial T}{\partial z}.$$

The boundary conditions are

$$\begin{gathered}u=L_1\frac{\partial u}{\partial z}, w=0, v=L_1\frac{\partial v}{\partial z}+\Omega r, T=L_2\frac{\partial T}{\partial z}+T_w \text{ at } z=0.\\ u\to 0, T\to T_\infty, v\to 0, p\to p_\infty \text{ as } z\to\infty.\end{gathered} \tag{6}$$

Here, L_1 and L_2 are the wall slip and thermal jump constant, respectively; Q_0 is the generation and absorption; $U_0=\Omega r$ is the free stream velocity; P is the pressure; σ_{tnf} is the electrical conductivity of ternary hybrid nanofluid; μ_{tnf} is the dynamic viscosity; ρ_{tnf} is the density; and (u, v, w) are the components of velocity.

The following variables are used to simplify Eqs 1–5 to the dimensionless system of ODEs:

$$\left.\begin{aligned}&\zeta=z\sqrt{\frac{U_0}{r\nu_f}},\ u=r\Omega f'(\zeta),\ w=-2\sqrt{\Omega\nu_f}g(\zeta),\ v=r\Omega g(\zeta),\\ &p=p_\infty-\Omega\mu_f P(\zeta),\ T=T_\infty+(T_w-T_\infty)\theta(\zeta).\end{aligned}\right\} \tag{7}$$

We get,

$$2\frac{\nu_{tnf}}{\nu_{hnf}}f'''-f'^2+g^2+4ff''-\frac{\rho_{hnf}}{\rho_{tnf}}M^2f'=0. \tag{8}$$

$$2\frac{\nu_{tnf}}{\nu_{hnf}}g''+2fg'-2f'g-\frac{\rho_{hnf}}{\rho_{tnf}}M^2g=0. \tag{9}$$

$$\frac{\nu_{tnf}}{\nu_{hnf}}f''+ff''-\frac{\rho_{hnf}}{\rho_{tnf}}\frac{\partial P}{\partial\zeta}=0. \tag{10}$$

$$\frac{\left(\rho C_p\right)_{hnf}}{\left(\rho C_p\right)_{tnf}}\left(\frac{k_{tnf}}{k_{hnf}}+Rd\right)\theta''+Pr f\theta'+Hs\theta=0. \tag{11}$$

TABLE 1 Investigational values of Al_2O_3, ZrO_2, CNT, and water Arif et al. (2022).

	$k\,(W/m.K)$	$\rho\,(kg/m^3)$	$C_p\,(J/kg.K)$	$\beta\,(1/K)$
Water	0.613	997.1	4,179	0.00021
Al_2O_3	40	3,970	765	0.00000508
ZrO_2	1.7	5,680	502	—
CNT	3,007.4	2,100	790	−0.000008

$$f(0)=0,\ g(0)=1+g'(0)\alpha,\ f'(0)=f''(0)\alpha,\ \theta(0)=1+\theta'(0)\beta.\quad f'\to 0,\ P\to 0,\ g\to 0,\ \theta\to 0 \text{ when } \zeta\to\infty. \tag{12}$$

Here, Pr is the Prandtl number, M is the magnetic constant, α is the slip velocity factor, β is the thermal slip constraint, and Rd is the thermal radiation term.

$$Pr=\frac{\mu_f\left(C_p\right)_f}{k_f},\ M^2=\frac{\sigma_{tnf}B_0^2}{\Omega\rho_f},\ \alpha=L_1\sqrt{\frac{\Omega}{\nu_f}},\ \beta=L_2\sqrt{\frac{\Omega}{\nu_f}},\ Rd=\frac{4\sigma T_\infty^3}{k^*k_f}. \tag{13}$$

The engineering interest quantities are

$$C_f=\frac{\sqrt{\tau_r^2+\tau_\theta^2}}{\rho_{tnf}(r\Omega)^2},\qquad Nu_r=\frac{k_{tnf}}{k_f}\frac{rq_w}{T_w-T_w}. \tag{14}$$

The dimensionless form of Eq. 14 is

$$\tau_w=\mu_{tnf}\left(\frac{\partial u}{\partial z}+\frac{\partial w}{\partial r}\right)\Big|_{z=0},\ \tau_\theta=\mu_{tnf}\left(\frac{\partial v}{\partial z}+\frac{\partial w}{\partial r}\right)\Big|_{z=0},\ q_w=-k_{tnf}\frac{\partial T}{\partial z}\Big|_{z=0}. \tag{15}$$

$$Re_r^{\frac{1}{2}}C_f=\frac{\mu_{hnf}}{\mu_{tnf}}\left(f''(0)^2+g'(0)^2\right)^{\frac{1}{2}}. \tag{16}$$

$$Re_r^{\frac{-1}{2}}Nu_r=\frac{-k_{hnf}}{k_{tnf}}Rd\theta'(0). \tag{17}$$

Here, $Re_r=\frac{2\Omega r^2}{\nu_f}$ is the local Reynolds number. Table 1 illustrates the experimental values of ternary nanoparticles and base fluid. Table 2 presented the mathematical model for trihybrid nanofluid.

Numerical solution

Many researchers have used different types of numerical and computational techniques to deal highly nonlinear PDEs (Zhao et al., 2018; Zhao et al., 2021a; Zhao et al., 2021b; Chu et al., 2022b; Jin et al., 2022; Nazeer et al., 2022; Rashid et al., 2022; Wang et al., 2022). The main steps, while dealing with the PCM method, are as follows (Shuaib et al., 2020a; Shuaib et al., 2020b; Bilal et al., 2022c):

Step 1: Simplify Eqs 8–11 to 1st order

$$\left.\begin{matrix}\lambda_1=f(\eta), & \lambda_2=f'(\eta), & \lambda_3=f''(\eta), & \lambda_4=g(\eta),\\ \lambda_5=g'(\eta), & \lambda_6=\theta(\eta), & \lambda_7=\theta'(\eta), & \lambda_8=p(\eta).\end{matrix}\right\} \tag{18}$$

By substituting Eq. 18 in Eqs 8–12, we get

$$2\frac{\nu_{tnf}}{\nu_{hnf}}\lambda_3'-\lambda_2^2+\lambda_4^2+4\lambda_2\lambda_3-\frac{\rho_{hnf}}{\rho_{tnf}}M^2\lambda_2=0. \tag{19}$$

$$2\frac{\nu_{tnf}}{\nu_{hnf}}\lambda_5'+2\lambda_1\lambda_5-2\lambda_2\lambda_4-\frac{\rho_{hnf}}{\rho_{tnf}}M^2\lambda_4=0. \tag{20}$$

TABLE 2 Thermochemical properties of ternary hybrid nanofluids Alharbi et al. (2022), Bilal et al. (2022b).

Viscosity	$\frac{\mu_{tnf}}{\mu_f}=\frac{1}{(1-\phi_{ZrO_2})^{2.5}(1-\phi_{Al_2O_3})^{2.5}(1-\phi_{CNT})^{2.5}}$
Density	$\frac{\rho_{tnf}}{\rho_f}=(1-\phi_{Al_2O_3})[(1-\phi_{Al_2O_3})\{(1-\phi_{CNT})+\phi_{CNT}\frac{\rho_{CNT}}{\rho_f}\}+\phi_{Al_2O_3}\frac{\rho_{Al_2O_3}}{\rho_f}]+\phi_{ZrO_2}\frac{\rho_{ZrO_2}}{\rho_f}$
Specific heat	$\frac{(\rho cp)_{tnf}}{(\rho cp)_f}=\phi_{ZrO_2}\frac{(\rho cp)_{ZrO_2}}{(\rho cp)_f}+(1-\phi_{ZrO_2})[(1-\phi_{Al_2O_3})\{(1-\phi_{CNT})+\phi_{CNT}\frac{(\rho cp)_{CNT}}{(\rho cp)_f}\}+\phi_{Al_2O_3}\frac{(\rho cp)_{Al_2O_3}}{(\rho cp)_f}]\}$
Thermal conduction	$\left.\begin{matrix}\frac{k_{tnf}}{k_{hnf}}=\left(\frac{k_{CNT}+2k_{hnf}-2\phi_{CNT}(k_{hnf}-k_{CNT})}{k_{CNT}+2k_{hnf}+\phi_{CNT}(k_{hnf}-k_{CNT})}\right),\frac{k_{hnf}}{k_{nf}}=\left(\frac{k_{Al_2O_3}+2k_{nf}-2\phi_{Al_2O_3}(k_{nf}-k_{Al_2O_3})}{k_{Al_2O_3}+2k_{nf}+\phi_{Al_2O_3}(k_{nf}-k_{Al_2O_3})}\right),\\ \frac{k_{nf}}{k_f}=\left(\frac{k_{ZrO_2}+2k_f-2\phi_{ZrO_2}(k_f-k_{ZrO_2})}{k_{ZrO_2}+2k_f+\phi_{ZrO_2}(k_f-k_{ZrO_2})}\right),\end{matrix}\right\}$
Electrical conductivity	$\frac{\sigma_{tnf}}{\sigma_{hnf}}=(1+\frac{3(\frac{\sigma_{CNT}}{\sigma_{hnf}}-1)\phi_{CNT}}{(\frac{\sigma_{CNT}}{\sigma_{hnf}}+2)-(\frac{\sigma_{CNT}}{\sigma_{hnf}}-1)\phi_{CNT}}),\ \frac{\sigma_{hnf}}{\sigma_{nf}}=(1+\frac{3(\frac{\sigma_{Al_2O_3}}{\sigma_{nf}}-1)\phi_{Al_2O_3}}{(\frac{\sigma_{Al_2O_3}}{\sigma_{nf}}+2)-(\frac{\sigma_{Al_2O_3}}{\sigma_{nf}}-1)\phi_{Al_2O_3}}),$ $\frac{\sigma_{nf}}{\sigma_f}=(1+\frac{3(\frac{\sigma_{ZrO_2}}{\sigma_f}-1)\phi_{ZrO_2}}{(\frac{\sigma_{ZrO_2}}{\sigma_f}+2)-(\frac{\sigma_{ZrO_2}}{\sigma_f}-1)\phi_{ZrO_2}}).$

10.3389/fenrg.2022.967307

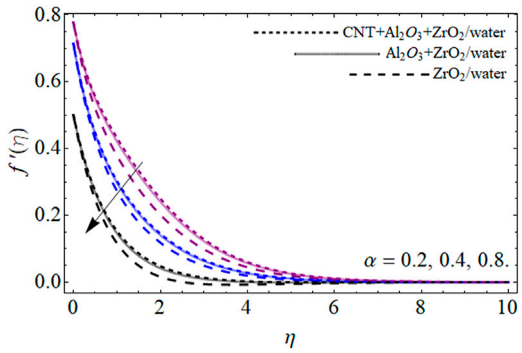

FIGURE 2
Velocity outlines $f'(\eta)$ versus velocity slip factor α.

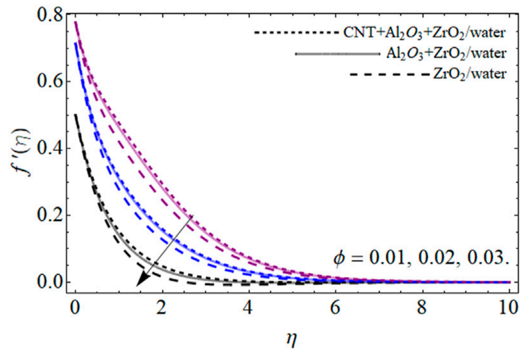

FIGURE 4
Velocity outlines $f'(\eta)$ versus ternary nanoparticles ϕ.

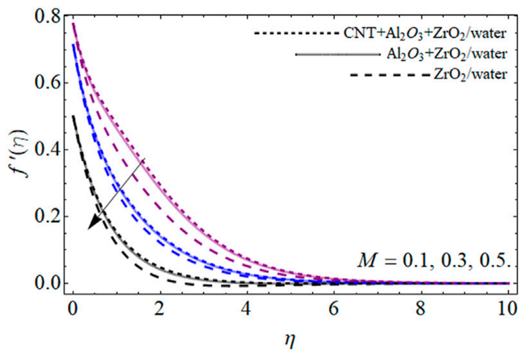

FIGURE 3
Velocity outlines $f'(\eta)$ versus magnetic term M.

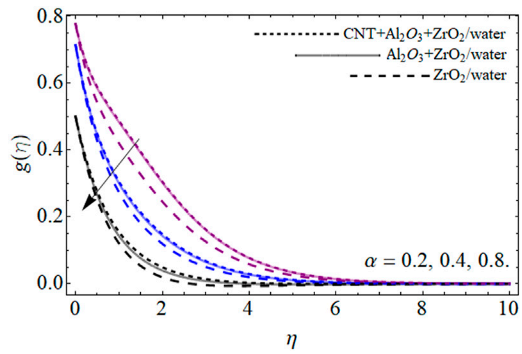

FIGURE 5
Velocity outlines $g(\eta)$ versus velocity slip factor α.

$$\frac{\nu_{tnf}}{\nu_{hnf}}\lambda_3 + \lambda_1\lambda_3 - \frac{\rho_{hnf}}{\rho_{tnf}}\lambda_8' = 0. \tag{21}$$

$$\frac{(\rho C_p)_{hnf}}{(\rho C_p)_{tnf}}\left(\frac{k_{tnf}}{k_{hnf}} + Rd\right)\lambda_7' + Pr\lambda_1\lambda_7 + Hs\lambda_6 = 0. \tag{22}$$

$$\lambda_1(0) = 0,\ \lambda_2(0) = \alpha\lambda_3(0),\ \lambda_4(0) = 1 + \alpha\lambda_5(0),\ \lambda_6(0) = 1 + \beta,\lambda_7(0),$$
$$\lambda_2 \to 0,\ g \to 0,\ \lambda_8 \to 0,\ \lambda_6 \to 0 \text{ when } \zeta \to \infty. \tag{23}$$

Step 2: Familiarizing parameter p in Eqs 19–22:

$$2\frac{\nu_{tnf}}{\nu_{hnf}}\lambda_3' - \lambda_2^2 + \lambda_4^2 + 4\lambda_2(\lambda_3 - 1)p - \frac{\rho_{hnf}}{\rho_{tnf}}M^2\lambda_2 = 0. \tag{24}$$

$$2\frac{\nu_{tnf}}{\nu_{hnf}}\lambda_5' + 2\lambda_1(\lambda_5 - 1)p - 2\lambda_2\lambda_4 - \frac{\rho_{hnf}}{\rho_{tnf}}M^2\lambda_4 = 0. \tag{25}$$

$$\frac{\nu_{tnf}}{\nu_{hnf}}\lambda_3 + \lambda_1(\lambda_3 - 1)p - \frac{\rho_{hnf}}{\rho_{tnf}}\lambda_8' = 0. \tag{26}$$

$$\frac{(\rho C_p)_{hnf}}{(\rho C_p)_{tnf}}\left(\frac{k_{tnf}}{k_{hnf}} + Rd\right)\lambda_7' + \mathrm{Pr}\lambda_1(\lambda_7 - 1)p + Hs\lambda_6 = 0. \tag{27}$$

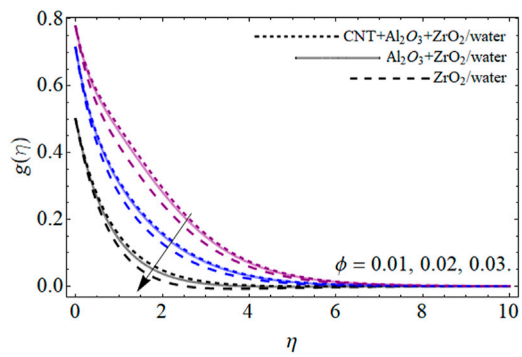

FIGURE 6
Velocity outlines $g(\eta)$ versus ternary nanoparticles ϕ.

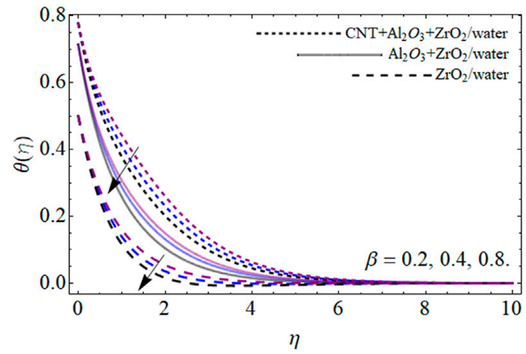

FIGURE 7
Energy outlines $\theta(\eta)$ versus thermal slip factor β.

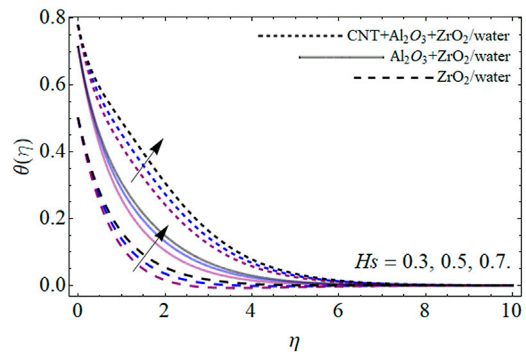

FIGURE 8
Energy outlines $\theta(\eta)$ versus heat source Hs.

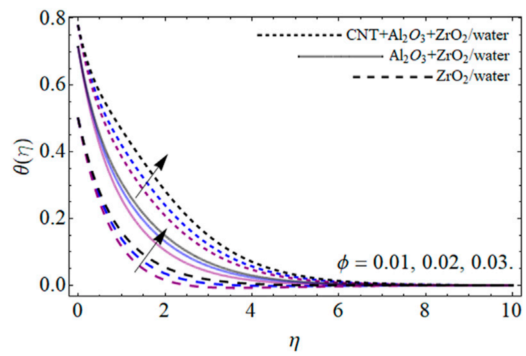

FIGURE 9
Energy outlines $\theta(\eta)$ versus ternary nanoparticles ϕ.

Step 3: Apply Cauchy principal and discretized Eqs 24–27.

After discretization, the obtained set of equations is computed through the MATLAB code of PCM.

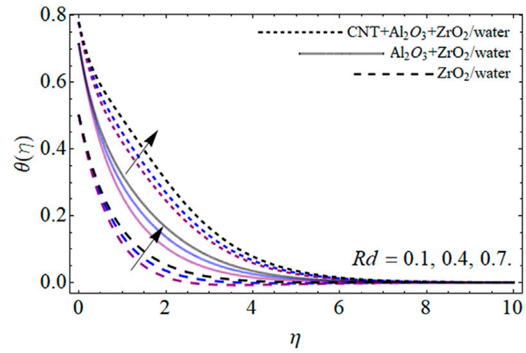

FIGURE 10
Energy outlines $\theta(\eta)$ versus thermal radiation Rd.

Results and discussion

This section elaborates the physics and trend behind each figure. The following statements are concluded from Figures 2–11.

Figures 2–4 revealed the axial velocity $f'(\eta)$ outlines versus velocity slip factor α, magnetic term M, and ternary nanoparticles ϕ, while Figures 5 and 6 display the radial velocity $g(\eta)$ outlines versus slip factor α and ternary nanoparticles ϕ, respectively. Figures 2 and 3 reported that the velocity contour diminishes with the influence of slip factor and magnetic term. The slip factor and magnetic force both resist the fluid field because the magnetic impact causes Lorentz strength, which opposes the fluid flow; hence, fluid velocity contour declines due to the increasing tendency of magnetic field and slip factor". Figure 4 shows that the dispersion of more quantity of ternary nanoparticles $(\phi = \phi_1 = \phi_2 = \phi_3)$ to water decelerates the fluid velocity. Physically, the inclusion of trihybrid nano composites to the base fluid enhances its average viscosity, which results in such retardation. Figures 5 and 6 present that the radial velocity also declines with the velocity slip factor and ternary nanoparticles. The upshot of trihybrid nanoparticles enhances the fluid viscosity, which resists the fluid velocity $g(\eta)$.

Figures 7–10 show the energy outlines versus the thermal slip factor β, heat source Hs, ternary nanoparticles ϕ, and thermal radiation Rd. Figure 7 expresses that the thermal slip factor reduces to the energy contour because slip effect minimizes the rate of frictional force, which results in reduction of energy field. Physically, the frictional force generates heat, so its reduction also decreases the temperature of fluid. Figure 8 illustrated that the heat generation and absorption term boost the energy profile. An additional energy is provided due to the rising effect of heat source, which elevates the energy profile. Figure 9 expresses that the addition of ternary nanoparticles enhances the temperature profile. The specific heat capacity of water (4,179 C_p (J/kg.K)) is much higher than that of Al_2O_3 (765 C_p (J/kg.K)), ZrO_2 (502 C_p (J/kg.K)), and CNT (790 C_p (J/kg.K)) nanoparticles. Therefore, the dispersion of these NPs to water lessens its average heat capacity, which fallouts in the elevation of energy outlines.

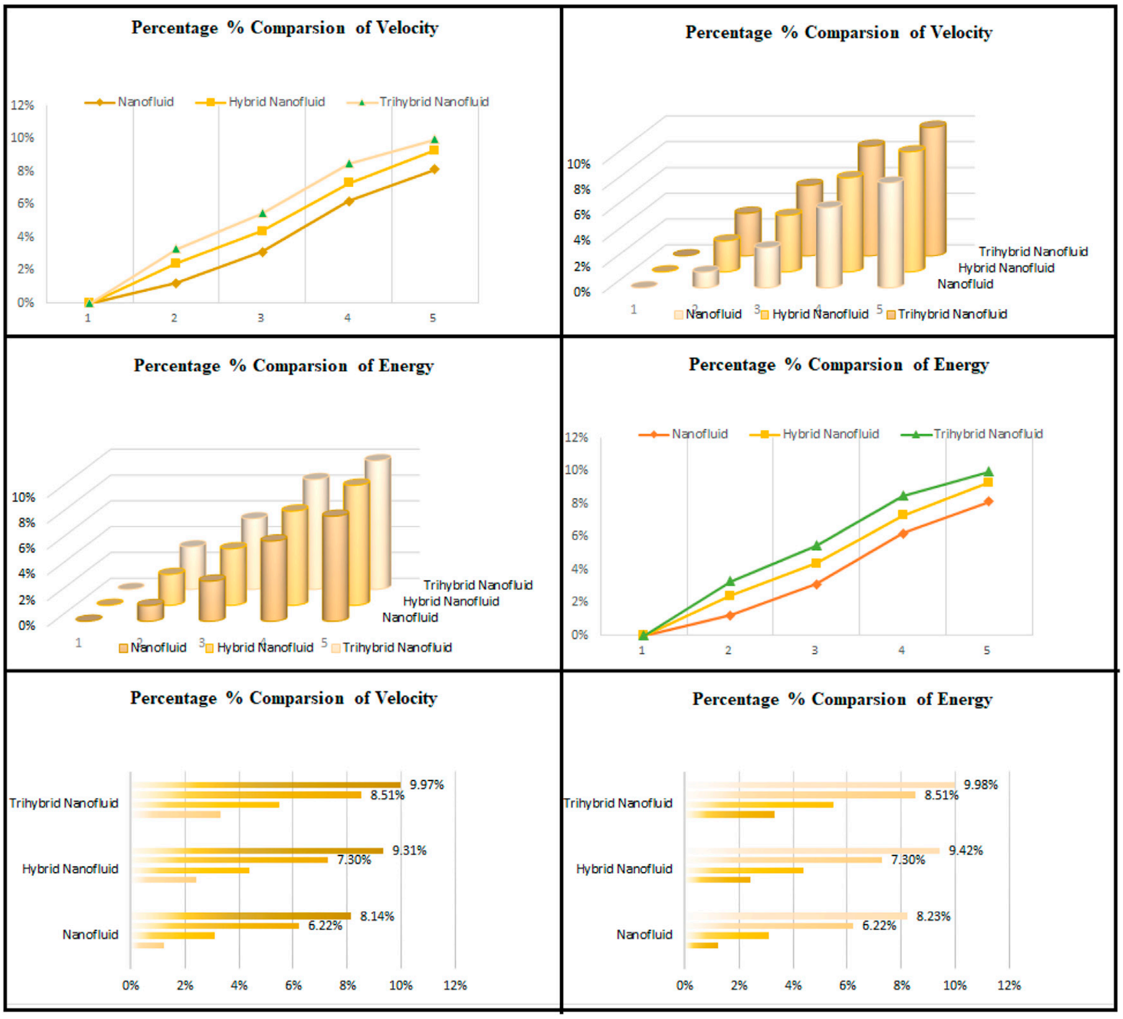

FIGURE 11
Percentage- and column-wise comparison of nanofluids.

Figure 10 displays that the upshot of radiation *Rd* term enhances the temperature contour. The impact of radiation term augments the energy of fluid, which causes in the inclination temperature contour.

Figure 11 demonstrates the comparative evaluation of nanofluid, hybrid, and ternary nanofluid. From all the subfigures of Figure 11, it can be noted that the ternary nanofluids have greater tendency to boost the energy transmission rate than hybrid and solo nanofluids.

Conclusion

We have examined the consequences of thermal radiation with slip boundary conditions and the uniform magnetic field on a steady 2D flow of trihybrid nanofluid over a rotating disc. The trihybrid nano composites are synthesized by the dispersion of Al_2O_3, ZrO_2, and CNT in water. A nonlinear system of PDEs is used to describe the phenomenon. The modeled equations are reduced to a nondimensional collection of ODEs using similarity substitution. The PCM methodology is used to estimate the nonlinear differential equations that resulted. The key findings are

- The axial velocity $f'(\eta)$ outlines are reducing with the influence of slip factor and magnetic term.
- The dispersion of ternary nanoparticles $(\phi = \phi_1 = \phi_2 = \phi_3)$ to water decelerates the fluid velocity.
- The radial velocity also declines with the velocity slip factor and ternary nanoparticles.
- The energy field declines with the increasing effects of thermal slip constraint.
- The influence of heat generation and absorption term boosts the energy profile.
- The addition of ternary nanoparticles magnifies the temperature profile.

- The fluid temperature augments with the effect of thermal radiation.
- The ternary nanofluid has higher thermal characteristics than simple and hybrid nanofluid.

Data availability statement

The original contributions presented in the study are included in the article/Supplementary Material; further inquiries can be directed to the corresponding author.

Author contributions

All authors listed have made a substantial, direct, and intellectual contribution to the work and approved it for publication.

Acknowledgments

The authors extend their appreciation to the Deanship of Scientific Research at King Khalid University, Saudi Arabia for funding this work through large groups under Grant No. RGP 2/32/43. The authors would like to thank the Deanship of Scientific Research at Umm Al-Qura University for supporting this work by Grant Code: 22UQU4331317DSR001.

Conflict of interest

The authors declare that the research was conducted in the absence of any commercial or financial relationships that could be construed as a potential conflict of interest.

Publisher's note

All claims expressed in this article are solely those of the authors and do not necessarily represent those of their affiliated organizations, or those of the publisher, the editors, and the reviewers. Any product that may be evaluated in this article, or claim that may be made by its manufacturer, is not guaranteed or endorsed by the publisher.

References

Ahmed, N., Khan, U., Mohyud-Din, S. T., Chu, Y. M., Khan, I., and Nisar, K. S. (2020). Radiative colloidal investigation for thermal transport by incorporating the impacts of nanomaterial and molecular diameters (dnanoparticles, dfluid): Applications in multiple engineering systems. *Molecules* 25 (8), 1896. doi:10.3390/molecules25081896

Ahmed, N., Khan, U., and Mohyud-Din, S. T. (2020). Hidden phenomena of MHD on 3D squeezed flow of radiative-H2O suspended by aluminum alloys nanoparticles. *Eur. Phys. J. Plus* 135 (11), 875. doi:10.1140/epjp/s13360-020-00870-2

Ahmed, N., Khan, U., Mohyud-Din, S. T., Khan, I., Murtaza, R., Hussain, I., et al. (2020). A novel investigation and hidden effects of MHD and thermal radiations in viscous dissipative nanofluid flow models. *Front. Phys.* 8, 75. doi:10.3389/fphy.2020.00075

Al-Mubaddel, F. S., Allehiany, F. M., Nofal, T. A., Alam, M. M., Ali, A., Asamoah, J. K. K., et al. (2022). Rheological model for generalized energy and mass transfer through hybrid nanofluid flow comprised of magnetized Cobalt ferrite nanoparticles. *J. Nanomater.* 2022, 1–11. doi:10.1155/2022/7120982

Algehyne, E. A., Alhusayni, Y. Y., Tassaddiq, A., Saeed, A., and Bilal, M. (2022). The study of nanofluid flow with motile microorganism and thermal slip condition across a vertical permeable surface. *Waves Random Complex Media*, 1–18. doi:10.1080/17455030.2022.2071501

Alharbi, K. A. M., Ahmed, A. E. S., Ould Sidi, M., Ahammad, N. A., Mohamed, A., El-Shorbagy, M. A., et al. (2022). Computational valuation of Darcy ternary-hybrid nanofluid flow across an extending cylinder with induction effects. *Micromachines* 13 (4), 588. doi:10.3390/mi13040588

Alhowaity, A., Bilal, M., Hamam, H., Alqarni, M. M., Mukdasai, K., Ali, A., et al. (2022). Non-Fourier energy transmission in power-law hybrid nanofluid flow over a moving sheet. *Sci. Rep.* 12 (1), 10406. doi:10.1038/s41598-022-14720-x

Alhowaity, A., Hamam, H., Bilal, M., and Ali, A. Numerical study of Williamson hybrid nanofluid flow with thermal characteristics past over an extending surface. *Heat. Trans.* doi:10.1002/htj.22616

Alrabaiah, H., Bilal, M., Khan, M. A., Muhammad, T., and Legas, E. Y. (2022). Parametric estimation of gyrotactic microorganism hybrid nanofluid flow between the conical gap of spinning disk-cone apparatus. *Sci. Rep.* 12 (1), 59. doi:10.1038/s41598-021-03077-2

Alsallami, S. A., Zahir, H., Muhammad, T., Hayat, A. U., Khan, M. R., Ali, A., et al. (2022). Numerical simulation of Marangoni Maxwell nanofluid flow with Arrhenius activation energy and entropy anatomization over a rotating disk. *Waves Random Complex Media*, 1–19. doi:10.1080/17455030.2022.2045385

Arif, M., Kumam, P., Kumam, W., and Mostafa, Z. (2022). Heat transfer analysis of radiator using different shaped nanoparticles water-based ternary hybrid nanofluid with applications: A fractional model. *Case Stud. Therm. Eng.* 31, 101837. doi:10.1016/j.csite.2022.101837

Bilal, M., Ahmed, A. E. S., El-Nabulsi, R. A., Ahammad, N. A., Alharbi, K. A. M., Elkotb, M. A., et al. (2022). Numerical analysis of an unsteady, electroviscous, ternary hybrid nanofluid flow with chemical reaction and activation energy across parallel plates. *Micromachines* 13 (6), 874. doi:10.3390/mi13060874

Bilal, M., Gul, T., Mouldi, A., Mukhtar, S., Alghamdi, W., Bouzgarrou, S. M., et al. (2022). Melting heat transition in a spinning flow of silver-magnesium oxide/engine oil hybrid nanofluid using parametric estimation. *J. Nanomater.* 2022, 1–13. doi:10.1155/2022/2891315

Bilal, M., Saeed, A., Gul, T., Kumam, W., Mukhtar, S., Kumam, P., et al. (2022). Parametric simulation of micropolar fluid with thermal radiation across a porous stretching surface. *Sci. Rep.* 12 (1), 2542. doi:10.1038/s41598-022-06458-3

Chu, Y. M., Bashir, S., Ramzan, M., and Malik, M. Y. (2022). Model-based comparative study of magnetohydrodynamics unsteady hybrid nanofluid flow between two infinite parallel plates with particle shape effects. *Math. Methods Appl. Sci.* doi:10.1002/mma.8234

Chu, Y. M., Nazir, U., Sohail, M., Selim, M. M., and Lee, J. R. (2021). Enhancement in thermal energy and solute particles using hybrid nanoparticles by engaging activation energy and chemical reaction over a parabolic surface via finite element approach. *Fractal Fract.* 5 (3), 119. doi:10.3390/fractalfract5030119

Chu, Y. M., Nazir, U., Sohail, M., Selim, M. M., and Lee, J. R. (2021). Enhancement in thermal energy and solute particles using hybrid nanoparticles by engaging activation energy and chemical reaction over a parabolic surface via finite element approach. *Fractal Fract.* 5 (3), 119. doi:10.3390/fractalfract5030119

Chu, Y. M., Shankaralingappa, B. M., Gireesha, B. J., Alzahrani, F., Khan, M. I., Khan, S. U., et al. (2022). Combined impact of Cattaneo-Christov double diffusion and radiative heat flux on bio-convective flow of Maxwell liquid configured by a stretched nano-material surface. *Appl. Math. Comput.* 419, 126883. doi:10.1016/j.amc.2021.126883

Elattar, S., Helmi, M. M., Elkotb, M. A., El-Shorbagy, M. A., Abdelrahman, A., Bilal, M., et al. (2022). Computational assessment of hybrid nanofluid flow with the influence of hall current and chemical reaction over a slender stretching surface. *Alexandria Eng. J.* 61 (12), 10319–10331. doi:10.1016/j.aej.2022.03.054

Gul, T., and Saeed, A. (2022). Nonlinear mixed convection couple stress tri-hybrid nanofluids flow in a Darcy–Forchheimer porous medium over a nonlinear stretching surface. *Waves Random Complex Media*, 1–18. doi:10.1080/17455030.2022.2077471

Hussain, S. M. (2022). Dynamics of ethylene glycol-based graphene and molybdenum disulfide hybrid nanofluid over a stretchable surface with slip conditions. *Sci. Rep.* 12 (1), 1751. doi:10.1038/s41598-022-05703-z

Iqbal, Z., Azhar, E., and Maraj, E. N. (2021). Performance of nano-powdersSiO2andSiCin the flow of engine oil over a rotating disk influenced by thermal jump conditions. *Phys. A Stat. Mech. its Appl.* 565, 125570. doi:10.1016/j.physa.2020.125570

Jin, F., Qian, Z. S., Chu, Y. M., and ur Rahman, M. (2022). On nonlinear evolution model for drinking behavior under Caputo-Fabrizio derivative. *jaac.* 12 (2), 790–806. doi:10.11948/20210357

Khan, U., Abbasi, A., Ahmed, N., and Mohyud-Din, S. T. (2017)., 39. Engineering Computations, 00. doi:10.1108/EC-04-2017-0149Particle shape, thermal radiations, viscous dissipation and joule heating effects on flow of magneto-nanofluid in a rotating system

Khan, U., Ahmed, N., and Mohyud-Din, S. T. (2020). Surface thermal investigation in water functionalized Al2O3 and γAl2O3 nanomaterials-based nanofluid over a sensor surface. *Appl. Nanosci.*, 1–11. doi:10.1007/s13204-020-01527-3

Kumar, M., and Mondal, P. K. (2022). Irreversibility analysis of hybrid nanofluid flow over a rotating disk: Effect of thermal radiation and magnetic field. *Colloids Surfaces A Physicochem. Eng. Aspects* 635, 128077. doi:10.1016/j.colsurfa.2021.128077

Li, Y. X., Muhammad, T., Bilal, M., Khan, M. A., Ahmadian, A., Pansera, B. A., et al. (2021). Fractional simulation for Darcy-Forchheimer hybrid nanoliquid flow with partial slip over a spinning disk. *Alexandria Eng. J.* 60 (5), 4787–4796. doi:10.1016/j.aej.2021.03.062

Lv, Y. P., Algehyne, E. A., Alshehri, M. G., Alzahrani, E., Bilal, M., Khan, M. A., et al. (2021). Numerical approach towards gyrotactic microorganisms hybrid nanoliquid flow with the hall current and magnetic field over a spinning disk. *Sci. Rep.* 11 (1), 8948. doi:10.1038/s41598-021-88269-6

Murtaza, S., Kumam, P., Ahmad, Z., Sitthithakerngkiet, K., and Ali, I. E. (2022). Finite difference simulation of fractal-fractional model of electro-osmotic flow of casson fluid in a micro channel. *IEEE Access* 10, 26681–26692. doi:10.1109/access.2022.3148970

Muzaidi, N. A. S., Fikri, M. A., Wong, K. N. S. W. S., Sofi, A. Z. M., Mamat, R., Adenam, N. M., et al. (2021). Heat absorption properties of CuO/TiO2/SiO2 trihybrid nanofluids and its potential future direction towards solar thermal applications. *Arabian J. Chem.* 14 (4), 103059. doi:10.1016/j.arabjc.2021.103059

Naveen Kumar, R., Mallikarjuna, H. B., Tigalappa, N., Punith Gowda, R. J., and Umrao Sarwe, D. (2022). Carbon nanotubes suspended dusty nanofluid flow over stretching porous rotating disk with non-uniform heat source/sink. *Int. J. Comput. Methods Eng. Sci. Mech.* 23 (2), 119–128. doi:10.1080/15502287.2021.1920645

Nazeer, M., Hussain, F., Khan, M. I., El-Zahar, E. R., Chu, Y. M., and Malik, M. Y. (2022). Theoretical study of MHD electro-osmotically flow of third-grade fluid in micro channel. *Appl. Math. Comput.* 420, 126868. doi:10.1016/j.amc.2021.126868

Palanisamy, R., Parthipan, G., and Palani, S. (2021). Study of synthesis, characterization and thermo physical properties of Al 2 O 3-SiO 2-TiO 2/H 2 O based tri-hybrid nanofluid. *Dig. J. Nanomater. Biostructures (DJNB)* 16 (3), 939.

Ramadhan, A. I., Azmi, W. H., Mamat, R., Hamid, K. A., and Norsakinah, S. (2019). Investigation on stability of tri-hybrid nanofluids in water-ethylene glycol mixture IOP Conference Series: Materials Science and Engineering. *IOP Conf. Ser. Mat. Sci. Eng.* 469 (1), 012068. doi:10.1088/1757-899x/469/1/012068

Ramzan, M., Saeed, A., Kumam, P., Ahmad, Z., Junaid, M. S., Khan, D., et al. (2022). Influences of Soret and Dufour numbers on mixed convective and chemically reactive Casson fluids flow towards an inclined flat plate. *Heat. Trans.* 51, 4393–4433. doi:10.1002/htj.22505

Rashid, S., Sultana, S., Karaca, Y., Khalid, A., and Chu, Y. M. (2022). Some further extensions considering discrete proportional fractional operators. *Fractals* 30 (01), 2240026. doi:10.1142/s0218348x22400266

Saeed, A., Bilal, M., Gul, T., Kumam, P., Khan, A., Sohail, M., et al. (2021). Fractional order stagnation point flow of the hybrid nanofluid towards a stretching sheet. *Sci. Rep.* 11 (1), 20429. doi:10.1038/s41598-021-00004-3

Safiei, W., Rahman, M. M., Yusoff, A. R., Arifin, M. N., and Tasnim, W. (2021). Effects of SiO2-Al2O3-ZrO2 tri-hybrid nanofluids on surface roughness and cutting temperature in end milling process of aluminum alloy 6061-T6 using uncoated and coated cutting inserts with minimal quantity lubricant method. *Arab. J. Sci. Eng.* 46 (8), 7699–7718. doi:10.1007/s13369-021-05533-7

Sahu, M., Sarkar, J., and Chandra, L. (2021). Steady-state and transient hydrothermal analyses of single-phase natural circulation loop using water-based tri-hybrid nanofluids. *AIChE J.* 67 (6), e17179. doi:10.1002/aic.17179

Sharma, K., Vijay, N., Mabood, F., and Badruddin, I. A. (2022). Numerical simulation of heat and mass transfer in magnetic nanofluid flow by a rotating disk with variable fluid properties. *Int. Commun. Heat Mass Transf.* 133, 105977. doi:10.1016/j.icheatmasstransfer.2022.105977

Shuaib, M., Shah, R. A., and Bilal, M. (2020). Variable thickness flow over a rotating disk under the influence of variable magnetic field: An application to parametric continuation method. *Adv. Mech. Eng.* 12 (6), 168781402093638. doi:10.1177/1687814020936385

Shuaib, M., Shah, R. A., Durrani, I., and Bilal, M. (2020). Electrokinetic viscous rotating disk flow of Poisson-Nernst-Planck equation for ion transport. *J. Mol. Liq.* 313, 113412. doi:10.1016/j.molliq.2020.113412

Sohail, M., Naz, R., and Abdelsalam, S. I. (2020). On the onset of entropy generation for a nanofluid with thermal radiation and gyrotactic microorganisms through 3D flows. *Phys. Scr.* 95 (4), 045206. doi:10.1088/1402-4896/ab3c3f

Sohail, M., Naz, R., Shah, Z., Kumam, P., and Thounthong, P. (2019). Exploration of temperature dependent thermophysical characteristics of yield exhibiting non-Newtonian fluid flow under gyrotactic microorganisms. *AIP Adv.* 9 (12), 125016. doi:10.1063/1.5118929

Sohail, M., Shah, Z., Tassaddiq, A., Kumam, P., and Roy, P. (2020). Entropy generation in MHD Casson fluid flow with variable heat conductance and thermal conductivity over non-linear bi-directional stretching surface. *Sci. Rep.* 10 (1), 12530. doi:10.1038/s41598-020-69411-2

Swain, K., Mebarek-Oudina, F., and Abo-Dahab, S. M. (2022). Influence of MWCNT/Fe3O4 hybrid nanoparticles on an exponentially porous shrinking sheet with chemical reaction and slip boundary conditions. *J. Therm. Anal. Calorim.* 147 (2), 1561–1570. doi:10.1007/s10973-020-10432-4

Ullah, I., Ali, R., Nawab, H., Uddin, I., Muhammad, T., Khan, I., et al. (2022). Theoretical analysis of activation energy effect on Prandtl–Eyring nanoliquid flow subject to melting condition. *J. Non-Equilibrium Thermodyn.* 47 (1), 1–12. doi:10.1515/jnet-2020-0092

Ullah, I. (2022). Heat transfer enhancement in Marangoni convection and nonlinear radiative flow of gasoline oil conveying Boehmite alumina and aluminum alloy nanoparticles. *Int. Commun. Heat Mass Transf.* 132, 105920. doi:10.1016/j.icheatmasstransfer.2022.105920

Ullah, I., Ullah, R., Alqarni, M. S., Xia, W. F., and Muhammad, T. (2021). Combined heat source and zero mass flux features on magnetized nanofluid flow by radial disk with the applications of Coriolis force and activation energy. *Int. Commun. Heat Mass Transf.* 126, 105416. doi:10.1016/j.icheatmasstransfer.2021.105416

Waini, I., Ishak, A., and Pop, I. (2022). Multiple solutions of the unsteady hybrid nanofluid flow over a rotating disk with stability analysis. *Eur. J. Mech. - B/Fluids* 94, 121–127. doi:10.1016/j.euromechflu.2022.02.011

Wang, F., Khan, M. N., Ahmad, I., Ahmad, H., Abu-Zinadah, H., Chu, Y. M., et al. (2022). Numerical solution of traveling waves in chemical kinetics: Time-fractional Fishers equations. *Fractals* 30 (2), 2240051–2240134. doi:10.1142/s0218348x22400515

Zhang, X. H., Algehyne, A., Ebrahem, A., Alshehri, G., Bilal, M., et al. (2021). The parametric study of hybrid nanofluid flow with heat transition characteristics over a fluctuating spinning disk. *Plos one* 16 (8), e0254457. doi:10.1371/journal.pone.0254457

Zhao, T. H., Khan, M. I., and Chu, Y. M. (2021). Artificial neural networking (ANN) analysis for heat and entropy generation in flow of non-Newtonian fluid between two rotating disks. *Math. Methods Appl. Sci.* doi:10.1002/mma.7310

Zhao, T. H., Wang, M. K., and Chu, Y. M. (2021). Concavity and bounds involving generalized elliptic integral of the first kind. *J. Math. Inequalities* 15 (2), 701–724. doi:10.7153/jmi-2021-15-50

Zhao, T. H., Wang, M. K., Zhang, W., and Chu, Y. M. (2018). Quadratic transformation inequalities for Gaussian hypergeometric function. *J. Inequal. Appl.* 2018 (1), 251. doi:10.1186/s13660-018-1848-y

Zhou, S. S., Bilal, M., Khan, M. A., and Muhammad, T. (2021). Numerical analysis of thermal radiative maxwell nanofluid flow over-stretching porous rotating disk. *Micromachines* 12 (5), 540. doi:10.3390/mi12050540